ANNALS OF "DUNAREA DE JOS" UNIVERSITY OF GALATI
MATHEMATICS, PHYSICS, THEORETICAL MECHANICS
FASCICLE II, YEAR XIII (XLIV) 2021, No. 1
DOI: https://doi.org/10.35219/ann-ugal-math-phys-mec.2021.1.10

Feed-Forward Back Propagation Network for the prediction of diabetic retinopathy disorder

Luminita Moraru[1,3], Simona Moldovanu[2,3], Andreea-Monica (Lăzărescu) Dincă[1,3]

[1]*Faculty of Sciences and Environment, Dunarea de Jos University of Galati, 111 Domneasca Str., 800201, Romania*
[2]*Faculty of Automation, Computers Sciences, Electronics and Electrical Engineering , Department of Computer Science and Information Technology, Dunarea de Jos University of Galati, 2 Stiintei Str., 800210, Romania*
[3]*The Modelling & Simulation Laboratory, Dunarea de Jos University of Galati, 47 Domneasca Str., 800008 Galati, Romania*

Abstract
Some retina disorders mainly involve some blocked blood clots so that, the retinal vessels change their structure, being unable to completely nourish the retina. For an accurate investigation of retina disorders, the extraction of the retinal vessel anatomical structures or lesions is the main task. This paper reports a combination of various features extracted from retinal images, that are further used to train a Feed-Forward Back Propagation Network (FFBPN) as a decision system. The main goal is determining the combination of the appropriate features for more accurate classification of healthy and diseased patients. To achieve this goal, 120 binary images covering both categories of patients that belong to the STARE (Structured Analysis of the Retina) database were analyzed. The input data are the number of ridges, bifurcation, and bridges for retinal vessel pattern recognition. The FFBPNs with 4, 8, 12, 16, and 20 neurons in the hidden layer are trained. The FFBNP architecture with 12 neurons in the hidden layer, using the *tansig* transfer function in the hidden layer and linear transfer function in the output layer provides the most appropriate model for retinopathy disease classification. The correlation between the number of ridges and bridges computed for healthy patients (as actual values) and the number of ridges and bridges for diabetic patients (as predicted values) provides the best result, a regression coefficient (R) of 0. 8575 and a mean-square error (MSE) of 0.00163.

Keywords: retinal images, bifurcation points, ridge, bridge, ANN, regression coefficient, mean square error.
.

I.INTRODUCTION

In recent years, extensive studies show that approximately 2.2 billion people have visual impairments [1]. A common eye condition is diabetic retinopathy. This involves damage to the retina caused by complications of diabetes. Diabetic retinopathy includes microaneurysms, hemorrhages, and macular edema that occur during diabetes for at least a few years. Possible complications associated with diabetic retinopathy include vitreous hemorrhage, detached retina, and glaucoma. Moreover, untreated or undetected in time, the retinopathy will lead to blindness.

Therefore, early recognition of changes in the retinal blood vessels can prevent vision loss. Sometimes, the early stage of eye disease cannot be observed by the patient or ophthalmologist; in such situations, diagnostic methods based on computer techniques can be very useful [2].
To identify and analyze various changes that occurred in the retinal vessels, biometric features such as bifurcation points, bridges, or ridges of a blood vessel are used [3].
Recent studies suggest that objective quantification of architectural changes in the retinal vascular network may be provided by morphological mathematic elements [4-7]. In 2014, Sajjan et al. [4] implemented an algorithm for extracting retinal blood vessels and detecting bifurcation points using

the Minutiae technique, in order to identify visual disturbances. The algorithm provided an accuracy higher than 80 %. S. Kaur et al. [5] proposed a blood vessel segmentation algorithm using artificial neural networks. The proposed algorithm was used for the early detection of diabetic retinopathy, with an image classification accuracy of around 95%. Pratt et al. [6], used convolutional neural networks and an algorithm that can learn to detect and classify bifurcations and crossings of blood vessels, with an accuracy of over 90%. M. Szymkowski et al. [7] have suggested the use of characteristic retinal points (details) for the purpose of medical diagnosis. The proposed method was evaluated using k-Nearest neighbors, k-Means and Support Vector Machines (SVM), as well as an approach based on specifying the number of details. The highest precision of 96.45% was obtained with the SVM.
ANNs are computational systems developed on the model of the neuronal cell of the human brain. The Feed-Forward Back Propagation Network (FFBPN) aims to learn and map the relationships between inputs and outputs, using weight and threshold values to obtain a minimum error. The ANN could provide an automated diagnosis of a retinal vessel with very good cost-effective and highly efficient care. Also, artificial intelligence algorithms provide automated detection of the retinal vessel without requiring any practicians to interpret retinal images. They can favor real-time clinical decision-making for the patients.
The current study uses five FFBPN models in order to classify retinal images belonging to healthy and retinal disease patients. An optimization operation is performed to obtain a maximum regression coefficient (R) and a minimum of the mean square error (MSE) values.

II. MATERIALS AND METHODS

This paper proposes the Minutiae extraction using morphological operator approach and, their subsequent processing using various FFBPN architectures for classification purposes. The main features of retinal images are the number of bifurcations, bridges, and ridges of the blood vessels. They are used to detect the anomalies present in the human retina automatically.

A. MORPHOLOGICAL OPERATORS

An erosion operation of binary image A by the structuring element B, is given by [8-11]:

$$A \Theta B = \left\{ \left(i, j \right) : B \cup A \right\} \tag{1}$$

where (i, j) denotes the center pixel of the structuring element and the structural element B is a disc with a radius of 5.

To overcome the limits of erosion followed by dilatation morphological operations related to the structuring element similarity with the shapes of the objects, the opening by reconstruction algorithm is used. This method optimally restores the original shapes of the objects after the erosion operation is performed [10, 11]. The opening by reconstruction of a gray-scale image A (x, y) using a gray-scale structuring element B, is defined as,

$$A \circ B \subseteq A \subseteq A \bullet B \tag{2}$$

where $A \circ B$ is the morphological opening operation defined as

$$A \circ B = \left(A \ominus B \right) \oplus B \tag{3}$$

and $A \bullet B$ is the morphological closing operation defined as

$$A \bullet B = (A \oplus B) \ominus B \tag{4}$$

$\oplus$ denotes the dilation operation and $\ominus$ the morphological erosion operation.
Skeletonization is a method for reducing foreground regions in a binary image. For structuring element B, the skeleton is the union of centers of maximal discs within a region X [12].
The n-the skeleton subset is:

$$S_n(X) = (X\Theta_n B) - \left[(X\Theta_n B) \circ B\right] \tag{5}$$

The operator Θ_n denotes n successive erosion operations. The skeleton is the union of all the skeleton subsets:

$$S(X) = \bigcup_{n=1}^{\infty} S_n(X) \tag{6}$$

Figure 1 presents the minutiae ridges, bifurcation, and bridges that are determined after skeletonization.

(a) (b) (c)

Fig. 1. Different types of minutiae, (a) bifurcation point; (b) bridge; (c) ridge.

B. HARDWARE AND SOFTWARE RESOURCES

The hardware platform is represented by a computer with the following configuration: Processor: Intel (R) Core (TM) i7-10870H CPU @ 2.20GHz 2.21 GHz, installed memory (RAM): 16.0 GB, system type: 64-bit operating system. For this study, MATLAB R2018a (The MathWorks, Natick, MA) was used as the programming medium with the ANN Artificial Neural Network toolkit.

120 binarized images were processed from the STARE database, 60 belonging to the healthy patients and 60 to the disease ones.

C. PROPOSED ALGORITHM

The pipeline of the algorithm is shown in figure 2. It determines three biometric characteristics of the retina, namely, the number of bifurcations, ridges, and bridges of the blood vessels. The biometric elements of interest were calculated and stored in a feature vector.

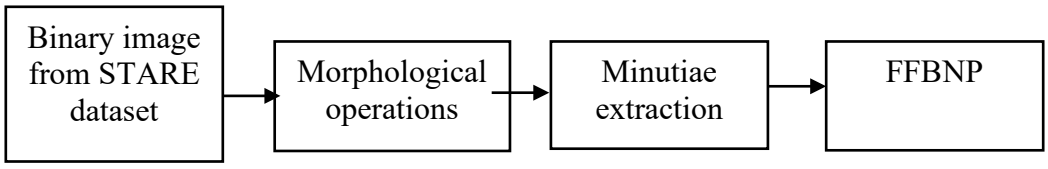

Fig.2. Algorithm for determining biometric elements

Figure 3 illustrates some results of the segmentation algorithm and minutiae extraction.

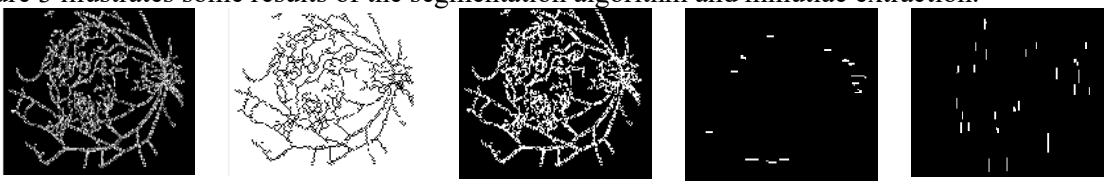

(a) (b) (c) (d) (e)

Fig. 3. The results of the retinal blood vessels segmentation and minutiae extraction. (a) Binary image showing the vessels map; (b) Thin image; (c) Determination of blood vessel bifurcations; (d) Detection of horizontal ridges; (e) Detection of vertical bridges.

D. FFBPN ARCHITECTURE

The FFBPN consists of an input layer, a hidden layer, and an output layer (fig. 4). The feature vectors containing the number of ridges, bifurcation, and bridges as well as their combinations are given as input to this neural network. The hidden layer consists of 4, 8, 12, 16, and 20 neurons, storing the history of previously trained characteristics. Given an input vector, the output vector will be compared with a desired, expected result. During the training stage, the FFBPN algorithm is used to update the weights and calculate the errors. Network parameters (i.e., number of hidden neurons, weights, biases) are defined during the training phase. In each training iteration, in the back propagation stage, a particular feature feeds the network in a straight direction, producing results at the output level. The difference between the actual / predicted results and the desired results is reduced using the mentioned algorithm. When the error of the desired output is minimal, the network weights are considered optimal. Thus, the stopping criterion correlates with the average square learning error. The parameters established during the training stage are further used for the classification stage for the test dataset.
The model was validated on 18 binary images. During the validation stage, only the number of neurons on the hidden layer has been changed to minimize MSE and maximize the R coefficient.
The proposed network was generated in the MATLAB programming environment, performing the following steps:

- Import input and output data into FFBPN
- Design the artificial neural network
- Divide the data into training, validation, and testing
- Compute R and MSE.

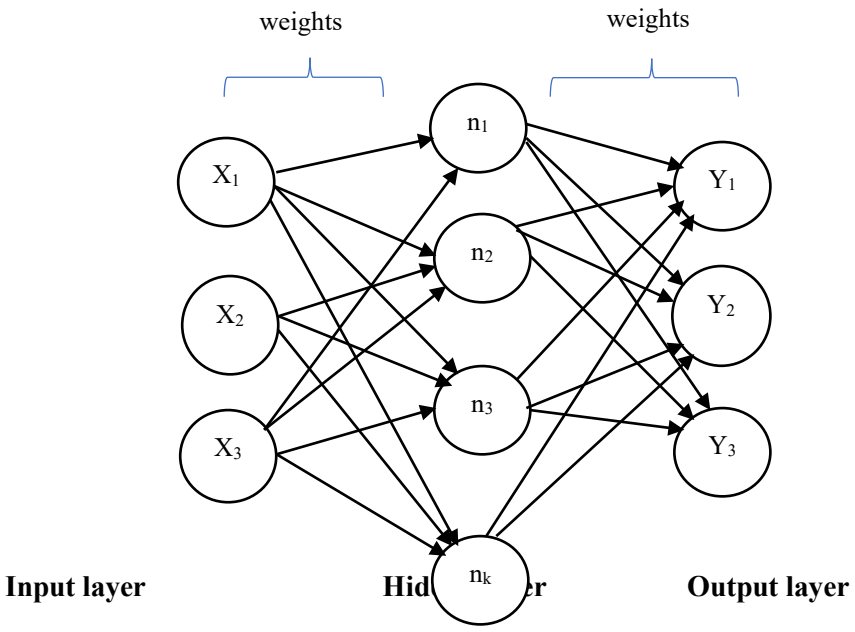

Fig. 4. The FFBPN architecture (k = 4, 8, 12, 16, 20 neurons). X_1, X_2, X_3 denote the input variables and the output variables Y_1, Y_2, Y_3 . Both sets consist of the number of ridges, bifurcation and bridges.

III. RESULTS AND DISCUSSION

The extracted biometric features (bifurcations, ridges, and bridges) are used for classification by employing a FFBPN.

The retinal images are divided into training (70%), testing (15%), and validation (15%). Table 1 shows the structure of the artificial neural network created.

Table 1. Characteristics of the design FFBPN

CHARACTERISTIC	NAME	EXPLANATIONS
Training algorithm	Feed-forward backpropagation	Type of artificial neural network
Training function	Trainlm	Levenberg-Marquardt backpropagation function
Transfer function	Tansig	Hyperbolic tangent sigmoid transfer function
Mean square error, regression coefficient	MSE, R	Performance of the neural network
Number of layers	2	Neural network architecture
The number of neurons on the hidden layer	4, 8, 12, 16, 20	
The total number of epochs	1000	

During the training stages, the following data representing the various combinations of minutiae V1, V2, V3, V4, V5, V6 are used (Table 2).

Table 2. Training option: Input data and Output data

TRAINING OPTIONS	INPUT DATA/healthy patients' data	TARGET/OUTPUT/DATA/ Retinopathy disease data
V1	Number of ridges	Number of ridges
V2	Number of bifurcations	Number of bifurcations
V3	Number of bridges	Number of bridges
V4	Number of ridges and bifurcations	Number of ridges and bifurcations
V5	Number of bifurcations and bridges	Number of bifurcations and bridges
V6	Number of ridges and bridges	Number of ridges and bridges

The training process of the proposed model automatically stops when an increase in MSE is obtained. A regression coefficient R close to 1 indicates a highly significant correlation between the obtained results and the desired ones. The FFBPN models with higher values of regression coefficients and lower MSE values proved to be more accurate for the declared goal.
The results obtained during the testing stage, using different FFBPN architectures are presented in Table 3.

Table 3. Prediction accuracy of the net's models during the testing stage

Training options	Number of neurons	MSE	R
V1	4	0.0991	0.7708
	8	0.103	0.74837
	12	0.0668	0.6947
	16	0.109	0.4692
	20	0.43	0.7471
V2	4	0.941	0.8317
	8	0.654	0.7715
	12	0.611	0.7924
	16	0.881	0.7181
	20	0.893	0.8073
V3	4	0.00168	0.4201
	8	0.00437	0.5355
	12	0.00173	0.7787
	16	0.00334	0.8532
	20	0.00173	0.7119
V4	4	0.12	0.7472
	8	0.0733	0.7432

	12	0.499	0.7471
	16	0.103	0.7837
	20	0.088	0.8584
V5	4	0.101	0.8218
	8	0.957	0.8106
	12	0.875	0.8294
	16	0.875	0.7895
	20	0.9	0.5881
V6	4	0.00341	0.661
	8	0.00356	0.7747
	12	0.00163	0.8575
	16	0.0113	0.7799
	20	0.00387	0.8583

Figures 5 and 6 illustrate the MSE and R values for all proposed models. The minutiae were analyzed with the proposed architecture, see Table 1. Figures 5(b) and 5(c) provide details of the MSE small values for V3 and V6 from figure 5 (a).

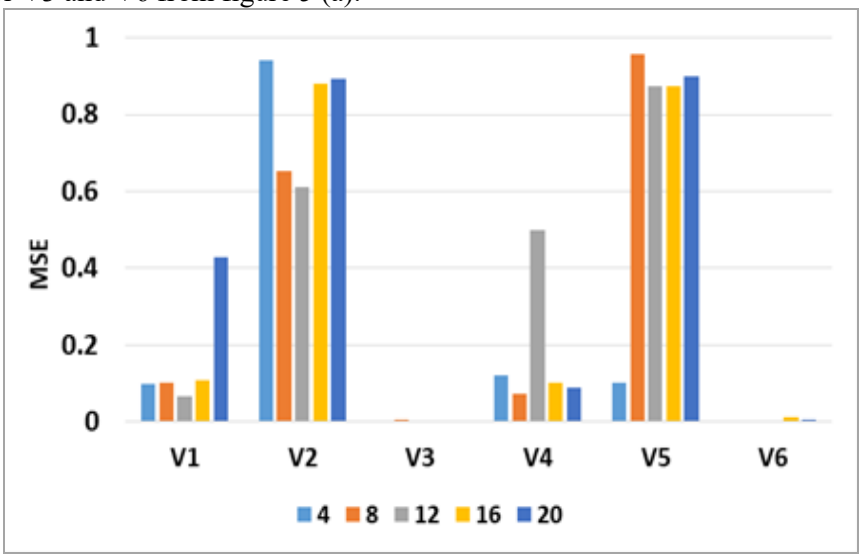

(a)

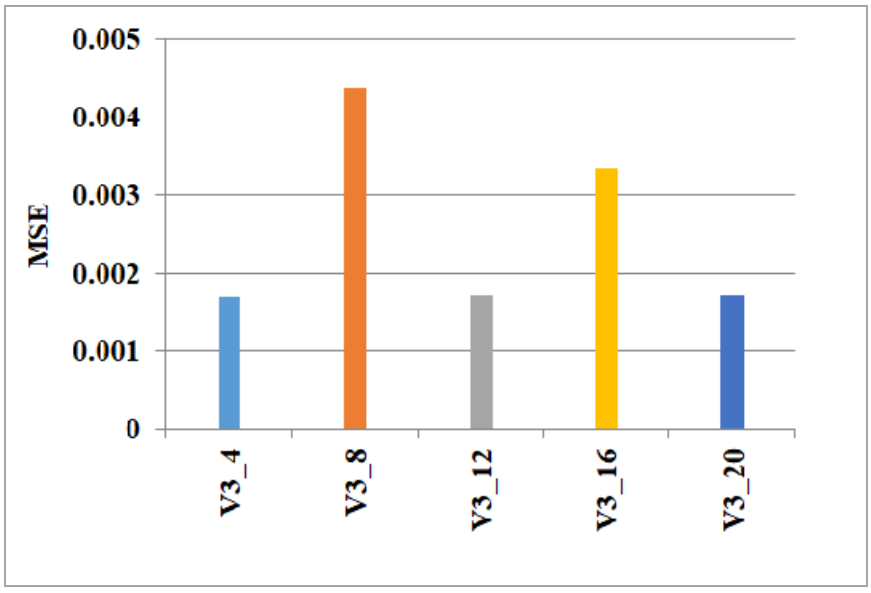

(b)

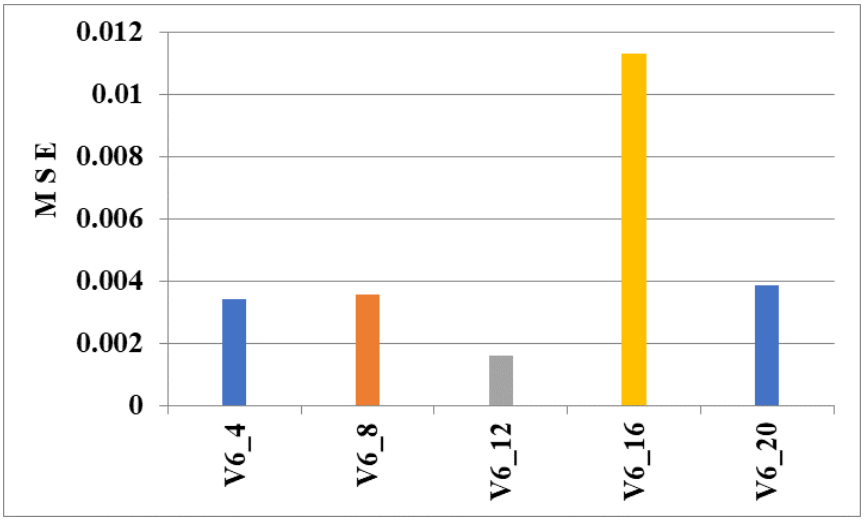

(c)

Fig. 5. MSE variation with the number of neurons in the training phase. (a) All variants; (b) V3 variant; (c) V6 variant

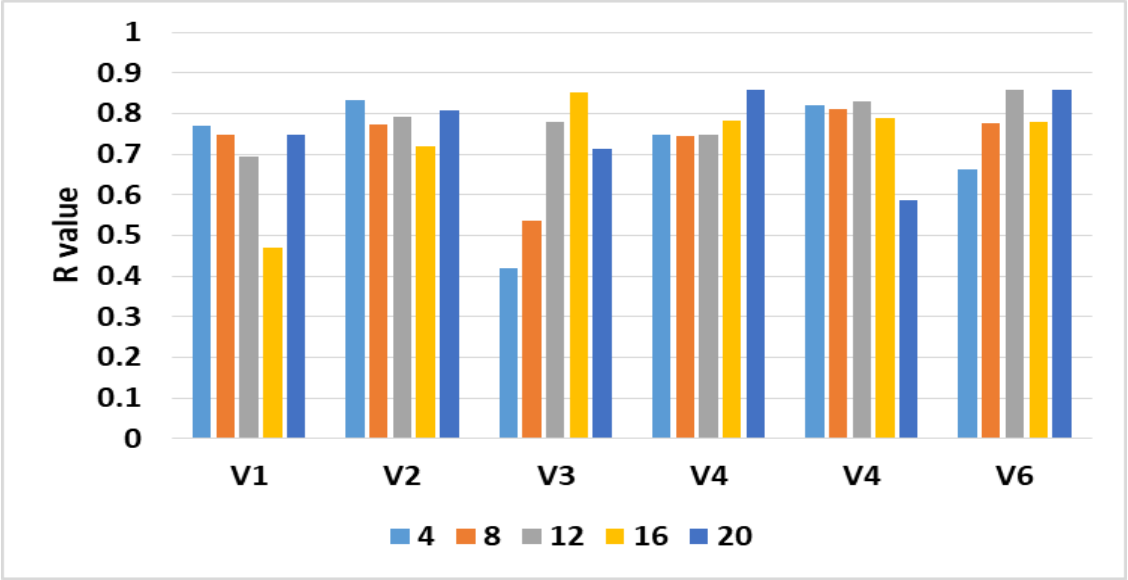

Fig. 6. Correlation coefficient R between actual and predicted values in the testing phase for different number of hidden neurons and working variants.

Generally, the best net architecture is selected based on the highest value of the correlation coefficient (R) and the lowest values of MSE. Comparing the results obtained using different FFBPN models where the input data were number of ridges, bifurcations, and ridges and their combinations received the following results: V3 (number of bridges as input data) and V6 (number of ridges and bridges as input data) variants yield R values close to one, while mean square errors (MSE) were found to be very low for 12 neurons in the hidden layer.

IV. CONCLUSION

In this study, six FFBPN models were used to develop a prediction model that can predict the combination of the appropriate features for more accurate classification of healthy and diseased patients. FFBPN neural network models were built with different numbers of neurons on the hidden layer. The final selected model was V6 (number of ridges and bridges as input data) and FFBPN with 12 neurons in the hidden layer. This model learns the relationship between the input and output parameters properly.

References

1. N. Rachburee, W. Punlumjeak, "An assistive model of obstacle detection based on deep learning: YOLOv3 for visually impaired people", International Journal of Electrical & Computer Engineering, Vol.11(4), pp.3434-3442, 2021
2. L. K.Singh, H. Garg, M. Khanna and R. S. Bhadoria "An enhanced deep image model for glaucoma diagnosis using feature-based detection in retinal fundus", ,Medical & Biological Engineering & Computing, vol 59, pp. 333–353, 2021
3. T.S. Sasikala and K. Sivasankar, "Minutiae Based Feature Level Fusion for Multimodal Biometrics", International Journal of Applied Engineering Research, vol 13(5), pp. 2763-2768, 2018
4. D. Sajjan, Dr. S. Kumar, "Extraction of Blood Vessels and Recognition of Bifurcation Points in Retinal Fundus Image", IJRSSET, vol. 1(5), pp. 1-2, 2014
5. K.S. Mann, S. Kaur, "Segmentation of retinal blood vessels using artificial neural networks for early detection of diabetic retinopathy", AIP Conference Proceedings 1836, pp.020026-020027, 2017
6. H. Pratt, B.M. Williams, JY Ku, C. Vas, E. McCann, B. Al-Bander, Y. Zhao, F. Coenen and Y. Zheng, "Automatic Detection and Distinction of Retinal Vessel Bifurcations and Crossings in Color Fundus Photography ", Journal of Imaging, vol 4(4), pp.12, 2017
7. M. Szymkowski, E. Saeed, M. Omieljanowicz, A. Omieljanowicz, K. Saeed, and Z. Mariak, "A Novelty Approach to Retina Diagnosing Using Biometric Techniques with SVM and Clustering Algorithms", J IEEEAccess, vol.8, pp. .125856, 2020
8. S.Z. Oo and A.S. Khaing, "Brain Tumor Detection and Segmentation using Watershed Segmentation and Morphological Operation", International Journal of Research in Engineering and Technology, vol.3(3), pp. 367-374, 2014.
9. S. Moldovanu, L. Moraru, A. Biswas, "Robust Skull-Stripping Segmentation based on Irrational Mask for Magnetic Resonance Brain Images", J Digit Imaging, vol.28(6), pp.738-747, 2015.
10. M. Ramesh, P. Priya, PM. Arabi, "A Novel Approach for Efficient Skull Stripping Using Morphological Reconstruction and Thresholding Techniques", International Journal of Research in Engineering and Technology, vol. 3(1), pp.96-101, 2014.
11. N. Senthilkumaran and C. Kirubakaran, "A Case Study on Mathematical Morphology Segmentation for MRI Brain Image", International Journal of Computer Science and Information Technologies, vol. 5(4), pp.5336-5340, 2014.
12. N. Neelima, Dr. A. Srikrishna, Dr. K. G. Rao, "Rank based Approach for Extracting Unit Pixel Width Skeleton", IOP Conference Series: Materials Science and Engineering 981, pp. 1-3, 2020